

## 4

7

10

14

16

18

Phone: +86-152-7081-8726



19   **Abstract:** Previous observational and chamber studies have highlighted the significant  
20   promoting effects of relative humidity (RH) or aerosol liquid water (ALW) on the  
21   formation of aerosol NACs. However, the applicability of this pattern needs further  
22   validation in large-scale field observations. This study presents the simultaneous  
23   investigation of the composition, abundance, origins of nitroaromatic compounds  
24   (NACs) in PM<sub>2.5</sub> across 11 Chinese cities during winter, with a focus on the key factors  
25   controlling NAC formation. Nitrophenols (NPs) and nitrocatechols (NCs) were  
26   identified as the main NAC groups, with their relative dominance varying by city.  
27   Higher total NAC concentrations were observed in northern cities, likely due to  
28   intensified coal and biomass burning. While secondary processes dominated wintertime  
29   NAC formation across all investigated cities, the average proportion of secondarily  
30   formed NACs was lower in the north (87%) than in the south (93%). This north-south  
31   disparity was more pronounced during polluted periods (82% vs. 96%). Furthermore,  
32   insignificant promoting effect of RH or ALW was found for most NACs except  
33   nitrosalicylic acids. The constraining effects from O<sub>3</sub>, ·OH, and solar radiation on NAC  
34   formation were stronger in northern China due to higher levels of light-absorbing air  
35   pollution, potentially offsetting the promoting effects of RH and ALW. These findings  
36   suggest that the RH- and ALW-promoted NAC formation may not be universally  
37   applicable in real atmospheric environments, where multi-factor interactions play a  
38   critical role. This study highlights the necessity of considering complex field conditions  
39   in future research on NAC formation mechanisms.

40  
41



## 42 1. Introduction

43 Nitrated phenol compounds are a class of aromatic organics characterized by the  
44 presence of both nitro ( $-\text{NO}_2$ ) and hydroxyl ( $-\text{OH}$ ) functional groups, which are  
45 ubiquitous in the atmospheric gas phase and particle phase (Cai et al., 2022; Li et al.,  
46 2020a; Huo et al., 2024). Key members of this nitroaromatic compound (NAC) class  
47 include nitrophenols (NPs), nitrocatechols (NCs), nitrosalicylic acids (NSAs),  
48 nitroguaiacols (NGs), and their derivatives (Li et al., 2020c; Huang et al., 2024). NACs  
49 are abundant constituents of atmospheric fine particulate matter ( $\text{PM}_{2.5}$ ) and are well  
50 recognized for their strong light-absorbing properties (Huang et al., 2025; Harrison et  
51 al., 2005; Wang et al., 2022). It has been reported that NAC species can contribute 4–  
52 50% or more to brown carbon light absorption (Mohr et al., 2013; Huang et al., 2024;  
53 Gu et al., 2022). Additionally, NACs are capable of strengthening the atmospheric  
54 oxidative capacity, as they promote the formation of HONO and OH radicals ( $\cdot\text{OH}$ )  
55 (Selimovic et al., 2020; Yang et al., 2021). These distinctive physicochemical properties  
56 ultimately influence regional air quality, radiative forcing, and climate dynamics  
57 (Harrison et al., 2005; Xiong et al., 2025; Liu et al., 2023b). In particular, NACs can  
58 also pose health risks due to their potential mutagenic and cytotoxic properties (Harrison  
59 et al., 2005; Hao et al., 2020). Thus, elucidating the abundances and main sources of  
60 NACs in urban aerosol particles and the key factors driving their formation is essential  
61 for advancing effective air pollution prevention efforts.

62 The molecular composition of aerosol NACs and the relative abundance of  
63 individual NAC species are strongly influenced by a combination of primary emission



64 sources and secondary formation processes (Li et al., 2020b; Xie et al., 2019; Ma et al.,  
65 2024; Macfarlane et al., 2025; Wang et al., 2022). Extensive observational studies have  
66 confirmed that NACs in aerosols can originate from primary emissions such as coal  
67 combustion, biomass burning, and vehicle exhaust (Zhang et al., 2023; Ma et al., 2024;  
68 Macfarlane et al., 2025; Chen et al., 2022; Lu et al., 2019). Furthermore, NACs can be  
69 secondarily formed through gas-phase and liquid-phase oxidation of various precursors,  
70 such as toluene, benzene, xylene, phenol, catechol, *m*-cresol, guaiacol, and methyl  
71 catechol, in the presence of nitrogen oxides (NO<sub>x</sub>), with their eventual distribution  
72 between gas and particle phases being significantly affected by gas-particle partitioning  
73 (Harrison et al., 2005; Wang and Li, 2021; Mayorga et al., 2021; Salvador et al., 2021;  
74 Vidović et al., 2019). Specifically, the formation of some NAC species in the particle  
75 phase involves nitration reactions of phenol, *o*-cresol, *o*-hydroxybenzoic acid, and *p*-  
76 hydroxybenzoic acid mediated by ·OH, NO<sub>3</sub>·, NO<sub>2</sub>·, N<sub>2</sub>O<sub>5</sub>, and ClNO<sub>2</sub> (Shi et al., 2023;  
77 Harrison et al., 2005; Wang and Li, 2021; Xiong et al., 2025). The atmospheric  
78 oxidation of catechol yields 4-nitrocatechol, a process initiated by ·OH and NO<sub>3</sub>·  
79 (Finewax et al., 2018). Similarly, methylnitrophenol and methylnitrocatechol can be  
80 produced via the photooxidation of *m*-cresol followed by subsequent nitration (Olariu  
81 et al., 2002). These well documented pathways in both laboratory experiments and field  
82 observations facilitate the conversion of volatile organic compounds (VOCs) into  
83 NACs with relatively low volatility, thereby substantially contributing to the formation  
84 of secondary organic aerosols (SOA) (Harrison et al., 2005; Liu et al., 2023b; Kroflič  
85 et al., 2021; Finewax et al., 2018; Macfarlane et al., 2025). In particular, the formation



86 of NACs is influenced by variations in ambient conditions such as relative humidity  
87 (RH), aerosol liquid water (ALW) concentration, and temperature (Xiong et al., 2025;  
88 Liu et al., 2023b; Guo et al., 2024). Among these, RH and ALW represent the most  
89 widely reported atmospheric variables affecting NAC formation (Xiong et al., 2025;  
90 Liu et al., 2023b). Nevertheless, the underlying RH- and/or ALW-related mechanisms  
91 controlling NAC production remain highly complex and not yet fully elucidated.

92 It is generally accepted that an increase in RH can elevate the concentration of  
93 ALW (Xu et al., 2023; Xu et al., 2020b; Nguyen et al., 2016). ALW not only promotes  
94 the partitioning of water-soluble gaseous organics into the particle phase but also  
95 functions as a reaction medium for aqueous-phase processes, which significantly  
96 increase SOA production (Sareen et al., 2017; Yang et al., 2024; Ma et al., 2025; Xu et  
97 al., 2022; Liu et al., 2023a). Recently, smog chamber experiments have suggested a  
98 water cluster catalysis mechanism underlying NAC formation, in which gaseous water  
99 molecules form proton-transfer bridges, increasing the reaction rate constants for the  
100 H-shift by approximately 8 to 17 orders of magnitude at 298 K compared to the scenario  
101 with liquid water (Xiong et al., 2025). However, previous field observations in cities  
102 such as Shanghai, Xi'an, and Beijing suggested that aerosol NAC levels did not exhibit  
103 a positive correlation with ALW (Huang et al., 2024; Liu et al., 2023b). Indeed, the  
104 mechanisms underlying the influence of RH and ALW on NAC formation remain a  
105 current research focus. However, to date, no large-scale synchronized observational  
106 studies in China have systematically investigated the linkages between aerosol NAC  
107 formation and RH or ALW.



108       Rapid urbanization and industrialization in China have intensified air pollution,  
109       especially during winter when biomass and coal combustion activities increase  
110       substantially (Ma et al., 2025; Xu et al., 2024b; Yang et al., 2025). Disparities in  
111       economic development levels among cities may consequently shape a unique spatial  
112       and temporal signature for NAC abundances, which are also modulated by factors like  
113       RH and ALW. In this study, we measured 9 typical NAC species in PM<sub>2.5</sub> samples  
114       simultaneously collected from 11 Chinese cities during winter. The objectives are: (1)  
115       to examine spatial variations in the concentration and composition of aerosol NACs; (2)  
116       to evaluate the relative contributions of primary emissions and secondary formation  
117       processes to aerosol NACs; and (3) to identify key factors governing the formation of  
118       NACs, with particular focus on the relationships between NAC abundances and RH or  
119       ALW in northern and southern China.

120

## 121   **2. Materials and methods**

### 122   **2.1. Sampling sites and sample collection**

123       The PM<sub>2.5</sub> sampling was conducted across 11 cities in China, geographically  
124       categorized into southern and northern groups based on the Qinling–Huaihe climatic  
125       boundary (**Figure S1**). The southern group consists of Guangzhou (GZ), Chengdu (CD),  
126       Guiyang (GY), Kunming (KM), Wuhan (WH), and Hangzhou (HZ). The northern sites  
127       encompass Lanzhou (LZ), Xi'an (XA), Beijing (BJ), Haerbin (i.e., Harbin; HEB), and  
128       Taiyuan (TY). The sampling campaign was carried out from December 10, 2017 to  
129       January 14, 2018. This period was characterized by a distinct south–north temperature



130 divide, with average air temperatures sustained above 4 °C in the southern cities  
131 generally below 2 °C in the northern cities (**Tables S1–S4**). It is noteworthy that biomass  
132 burning activities are relatively active during winter in both southern and northern  
133 Chinese cities (Yang et al., 2025; Huang et al., 2024).

134 PM<sub>2.5</sub> samples were acquired using a high-volume air sampler (KC-1000, Laoying,  
135 China) operated at a constant flow rate of  $1.05 \pm 0.03 \text{ m}^3 \text{ min}^{-1}$ , with prebaked quartz  
136 fiber filters (Pallflex, Pall Corporation, USA) serving as the collection medium.  
137 Sampling was conducted simultaneously across 11 observation sites on a 2- to 3-day  
138 frequency cycle, with each sampling event lasting approximately 24 hours. Field blank  
139 samples were prepared at each site by mounting filters in an identical but non-operating  
140 air sampler. This campaign yielded a total of 154 filter samples, which were  
141 subsequently preserved at –30 °C. Concurrent meteorological data (e.g., temperature  
142 and RH) and air pollutant concentrations (e.g., SO<sub>2</sub>, NO<sub>x</sub>, CO, and O<sub>3</sub>) recorded during  
143 the sampling dates were obtained from nearby monitoring stations. The solar shortwave  
144 radiation (SR) data were obtained from National Meteorological Information Center,  
145 China Meteorological Administration (<http://data.cma.cn/>). In addition, a PM<sub>2.5</sub>  
146 concentration threshold of  $75 \mu\text{g m}^{-3}$  was applied to differentiate between clean and  
147 polluted days throughout the sampling campaign (Xu et al., 2024b; Zhang and Cao,  
148 2015).

149

## 150 2.2. Chemical analysis and parameter calculation



151 The protocol for extracting NACs from filter samples followed an optimized  
152 sample preparation workflow (Frka et al., 2022; Huang et al., 2024; Ma et al., 2024;  
153 Ma et al., 2025). Briefly, methanol was used for extracting the filter samples, after  
154 which the extract was filtered through a 0.22  $\mu\text{m}$  polytetrafluoroethylene syringe filter  
155 (CNW Technologies GmbH). Subsequently, the filtrate was concentrated to near-  
156 dryness using a gentle stream of nitrogen gas. The residue was reconstituted by adding  
157 300  $\mu\text{L}$  of ultrapure water ( $\sim 18.2 \text{ M}\Omega \text{ cm}$ ), followed by mixing and centrifugation. The  
158 final supernatant was injected for analysis using ultra-high-performance liquid  
159 chromatography-tandem mass spectrometry (UPLC-MS/MS, Waters, USA).  
160 Chromatographic separation was achieved on an ACQUITY UPLC HSS T3 analytical  
161 column (2.1 mm  $\times$  100 mm, 1.8  $\mu\text{m}$ ; Waters, USA).

162 Nine NAC species were targeted for quantification, including 4-nitrophenol (4NP),  
163 2,4-dinitrophenol (2,4DNP), 3-methyl-4-nitrophenol (3M4NP), 2-methyl-4-  
164 nitrophenol (2M4NP), 4-nitrocatechol (4NC), 4-methyl-5-nitrocatechol (4M5NC), 5-  
165 nitrosalicylic acid (5NSA), 3-nitro-salicylic acid (3NSA), and 4-nitroguaiacol (4NG).  
166 For the standard reference materials, recoveries fell within the range of 94% to 105%.  
167 None of these NACs were detectable in blank samples when analyzed using the  
168 identical measurement protocol. Furthermore, two typical anthropogenic organosulfate  
169 markers (i.e.,  $\text{C}_8\text{H}_{17}\text{O}_4\text{S}^-$  and  $\text{C}_5\text{H}_7\text{O}_6\text{S}^-$ ) were also measured via a comparable  
170 analytical approach (Yang et al., 2023; Yang et al., 2024; Xu et al., 2025). Detailed  
171 procedures for the identification and quantification of these organosulfate species have  
172 been described in our previous publications (Yang et al., 2023; Yang et al., 2024).





173 Levoglucosan (LGA) was additionally identified based on a similar UPLC-MS method  
 174 outlined above (Ma et al., 2025).

175 The analytical procedure for inorganic ions in PM<sub>2.5</sub> samples involved the  
 176 ultrapure water-based extraction via a ~4 °C ultrasonic bath (Gui et al., 2025; Xu et al.,  
 177 2024a). After extraction, the solutions were passed through a polytetrafluoroethylene  
 178 syringe filter. Analysis was conducted via ion chromatography (Dionex Aquion,  
 179 Thermo Scientific, USA) to measure the concentrations of Mg<sup>2+</sup>, Ca<sup>2+</sup>, Na<sup>+</sup>, Cl<sup>-</sup>, SO<sub>4</sub><sup>2-</sup>,  
 180 NO<sub>3</sub><sup>-</sup>, NH<sub>4</sub><sup>+</sup>, and K<sup>+</sup> (Xu et al., 2020a; Gui et al., 2024). The concentration of ALW and  
 181 the pH value were estimated by running the ISORROPIA-II thermodynamic model in  
 182 forward mode under the assumption of a metastable state, following methodologies  
 183 well-documented in our previous work (Yang et al., 2024; Ma et al., 2025; Gui et al.,  
 184 2025). In addition, the non-sea-salt fractions of K<sup>+</sup> (nss-K<sup>+</sup>) and Cl<sup>-</sup> (nss-Cl<sup>-</sup>) were  
 185 derived by subtracting 0.038 and 1.727 times the Na<sup>+</sup> concentration from the total  
 186 concentration of each respective ion (Boreddy and Kawamura, 2015; Morales et al.,  
 187 1998). In addition, the levels of ambient ·OH were estimated using the empirical  
 188 formula proposed by Ehhalt and Rohrer (2000), which was detailed in our previous  
 189 publications (Liu et al., 2023a; Xu et al., 2024a).

190

### 191 **3. Results and discussion**

#### 192 **3.1. Spatial characteristics of NAC concentration and composition in PM<sub>2.5</sub>**

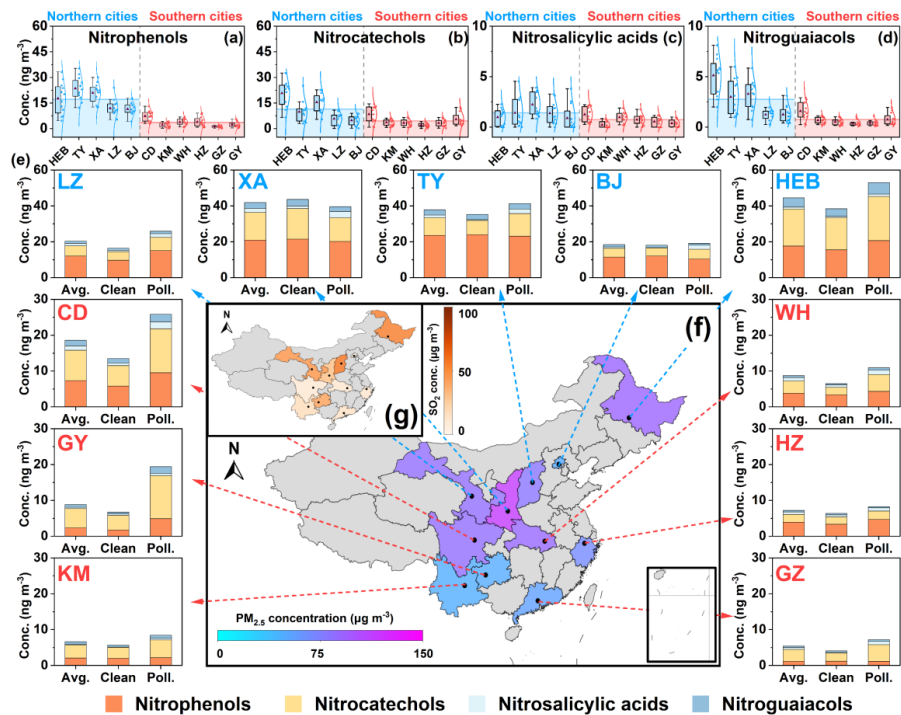
193 **Figure 1a–d** shows the average concentration distributions of different NAC  
 194 groups in PM<sub>2.5</sub> samples collected from 11 cities across China, along with a comparative



195 analysis of their levels in southern and northern cities. NACs are categorized into four  
 196 groups, including nitrophenols (NPs), nitrocatechols (NCs), nitrosalicylic acids (NSAs),  
 197 and nitroguaiacols (NGs) (**Table S1–S4**). On average, nitrophenols and nitrocatechols  
 198 are the two dominant categories, constituting approximately  $43.75 \pm 14.33\%$  and  $42.44$   
 199  $\pm 13.46\%$  of the total measured NACs in the investigated cities, respectively (**Figure**  
 200 **S2** and **Table S1–S2**). Nitrosalicylic acids and nitroguaiacols represent relatively minor  
 201 proportions, account for only  $6.12 \pm 2.99\%$  and  $7.69 \pm 1.80\%$  of the total NACs,  
 202 respectively. The highest average concentration of total nitrophenols was observed in  
 203 TY, while the peak average level of total nitrocatechols was recorded in HEB. The  
 204 lowest average total nitrophenol concentration was found in GZ, whereas HZ exhibited  
 205 the lowest average total nitrocatechol level. Similarly, the average total abundances of  
 206 nitrosalicylic acids and nitroguaiacols also showed significant spatial variations, with  
 207 the highest mean values recorded in XA and HEB, respectively, and the lowest mean  
 208 values in KM and HZ, respectively. Although neither nitrophenols nor nitrocatechols  
 209 reached their individual peak concentrations in XA, the average total NAC  
 210 concentration was the highest in this city (**Figure 1e** and **Table S1–S2**). Across all the  
 211 investigated cities, the average concentration of total NACs was  $20.09 \text{ ng m}^{-3}$ , ranging  
 212 from  $5.55 \text{ ng m}^{-3}$  to  $44.87 \text{ ng m}^{-3}$ . This falls within the range reported in previous  
 213 studies (Huang et al., 2024; Liu et al., 2023b; Gu et al., 2022; Cai et al., 2022; Li et al.,  
 214 2016). The second-highest total average NACs concentration was observed in HEB,  
 215 followed by TY, XA, LZ, CD, BJ, GY, HW, HZ, KM, and GZ. For all four categories  
 216 of NACs as well as the total NAC concentration, their average levels were consistently



217 higher in northern cities than in southern cities (**Figure 1a-d** and **Figure S3**). This  
218 spatial pattern is similar to that of PM<sub>2.5</sub> and SO<sub>2</sub> (typical pollutants emitted from coal  
219 combustion) (**Figure 1f,g**). Many previous studies have documented that the abundance  
220 of NACs in winter aerosols can be significantly influenced by primary emissions such  
221 as coal and biomass burning (Wang et al., 2017; Wang et al., 2020; Huang et al., 2023).  
222 Thus, the north-south gradient in NAC concentrations is likely closely associated with  
223 divergent air pollution levels (as indicated by PM<sub>2.5</sub> levels) between northern and  
224 southern China, partly driven by differences in coal combustion and biomass burning  
225 intensity.



227  
228 **Figure 1.** Box and whisker plots (a-d) showing the variations in the mean



229 concentrations of different NAC groups in PM<sub>2.5</sub> collected in 11 Chinese cities. The  
 230 boxes represent the interquartile range (25th to 75th percentiles). The whiskers extend  
 231 from the 5th to the 95th percentiles. The solid triangles inside boxes indicate the mean.  
 232 (e) Average concentration distributions of detected NACs in PM<sub>2.5</sub> during clean and  
 233 polluted days in winter across 11 Chinese cities. The color blocks in the panels (f) and  
 234 (g) represent the spatial variations in PM<sub>2.5</sub> and SO<sub>2</sub> pollution levels, respectively,  
 235 across the sampled cities during the study period. The map was obtained from  
 236 ©MeteoInfoMap (Chinese Academy of Meteorological Sciences, China).

237

238 Among nitrophenols, 4-nitrophenol (4NP) was the most abundant species,  
 239 accounting for  $63.21 \pm 8.07\%$  of the total measured nitrophenols in China during winter  
 240 (**Figure S4** and **Table S1–S4**). Previous studies characterizing NACs in biomass  
 241 burning emissions have reported 4NP as an important emitted species (Huang et al.,  
 242 2024; Wang et al., 2020; Wang et al., 2017). 4-nitrocatechol (4NC) was the dominant  
 243 species among nitrocatechols. The average concentration of 4NC across all cities was  
 244  $7.55 \pm 6.90 \text{ ng m}^{-3}$ , representing  $40.67 \pm 12.89 \%$  of total NACs. The emission factors  
 245 for 4NC from coal combustion varied widely based on geological maturity, ranging  
 246 from 8 to  $3487 \text{ } \mu\text{g kg}^{-1}$  (Huang et al., 2023). In contrast, the emission factors of 4NP  
 247 from the same coal sources were significantly lower, generally below  $14 \text{ } \mu\text{g kg}^{-1}$  (Huang  
 248 et al., 2023). Furthermore, the average emission factor for nitrocatechols from the  
 249 combustion of biomass materials was also substantial, measured at  $26.6 \pm 5.40 \text{ } \mu\text{g kg}^{-1}$   
 250 (Huang et al., 2023). These findings indicate that coal and biomass burning during



251 winter may significantly contribute to the abundance of NACs in urban aerosols across  
252 China, particularly exacerbating NACs pollution in northern cities.

253 The mass concentration fractions of various NACs were further compared between  
254 clean and polluted days (**Figure 1e**). It was observed that the dominant NAC groups  
255 (i.e., nitrophenols and nitrocatechols) in PM<sub>2.5</sub> remained consistently predominant  
256 across all cities from clean to polluted periods, without being superseded by other NAC  
257 species. This pattern suggests that the main emission sources of aerosol NACs in these  
258 urban areas may not have undergone significant changes during pollution periods. In  
259 most cities, including LZ, HEB, CD, WH, GY, HZ, KM, and GZ, the average  
260 concentrations of total NACs and dominant NAC groups showed an increasing trend  
261 from clean to polluted periods (**Figure 1e** and **Table S1–S4**). In contrast, cities such as  
262 XA, TY, and BJ exhibited a decreasing trend in the concentrations of main NAC groups  
263 (i.e., nitrophenols). It should be noted that nitrophenols were not the primary species in  
264 GZ, and their average concentrations did not show an increasing trend from clean to  
265 polluted periods. As important contributors to haze formation, NACs would be  
266 expected to accumulate under polluted air conditions. Thus, the observed decrease in  
267 the abundance of some NAC groups on polluted days (typically associated with calm  
268 and stable weather conditions) in several cities suggests that the formation of NAC  
269 compounds may also be constrained by specific factors such as photolysis process (Liu  
270 et al., 2024; Yang et al., 2021), varied RH and ALW levels (Xiong et al., 2025; Liu et  
271 al., 2023b), and unfavorable atmospheric oxidation capacity (Wang and Li, 2021).  
272 These influencing factors will be further discussed in later sections. In general, the



273 concentration and composition of NACs varied spatially (**Figure 1** and **Figure S2**),  
 274 which may be attributed to spatial differences in precursor sources, emission intensities,  
 275 and the key factors influencing aerosol NAC formation.

276

### 277 **3.2. Temporal variations of NACs and their potential origins**

278 **Figure 2** shows the time series of concentrations of various NACs and key  
 279 chemical components in winter PM<sub>2.5</sub> across northern and southern China. In northern  
 280 China, the highest total NP concentration was observed in TY, whereas the highest total  
 281 NC event occurred in HEB (**Figure 2a,c,e**). In HEB, XA, and BJ, total NPs and total  
 282 NCs exhibited similar variation trends (linear regression,  $P < 0.05$ ), implying  
 283 potentially similar sources for aerosol NPs and NCs. In TY and LZ, total NPs and total  
 284 NCs also showed consistent variation patterns during most observation periods.  
 285 Furthermore, NGs were significantly ( $P < 0.05$ ) correlated with total NCs in all regions  
 286 except TY and LZ. In southern cities, the most severe NACs pollution events were  
 287 recorded in CD (**Figure 2d,d,f**), which may be attributed to the city's basin topography  
 288 that hinders pollutant dispersion (Liao et al., 2017). With the exception of GZ, major  
 289 NAC species in southern cities exhibited similar temporal trends. In GZ, several  
 290 anomalously high NC cases likely led to inconsistent variation patterns among different  
 291 NAC groups. Overall, the temporal variation trends of major NAC groups were highly  
 292 consistent across most Chinese cities, indicating that the sources of different NACs  
 293 during winter may be similar in each city.

294

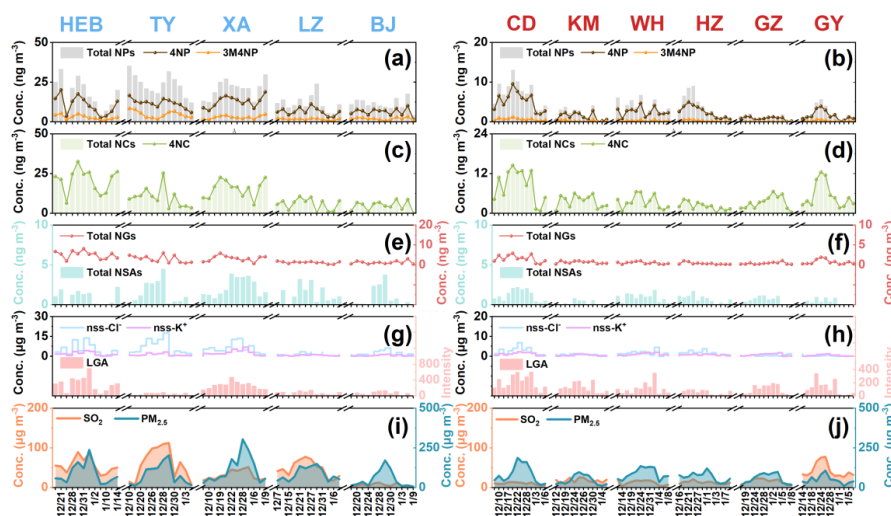


**Figure 2.** Temporal variations in (a–f) various NAC species and (g–l) key parameters in 11 Chinese cities.

Comparison of the temporal variation patterns (**Figure 2g–j**) and correlations of

NACs against various combustion source tracers (**Figure 3a,b**) enabled the identification of their potential sources in the different cities (Huang et al., 2024; Cai et al., 2022; Wang et al., 2019; Kahnt et al., 2013). In northern cities, one or more NAC species showed consistent variation trends with indicators of biomass burning or coal combustion, including LGA,  $\text{nss-K}^+$ ,  $\text{SO}_2$ ,  $\text{nss-Cl}^-$ , and  $\text{C}_8\text{H}_{17}\text{O}_4\text{S}^-$  (Kahnt et al., 2013; Ma et al., 2025; Yang et al., 2025; Yang et al., 2023) (**Figure 2g,i** and **Figure 3a**). The highest frequency of significant positive correlations between various NACs and biomass or coal combustion tracers (i.e., the number of orange-red rectangles marked with asterisks in the **Figure 3c**) was observed in HEB ( $n = 17$ ), followed by LZ ( $n = 12$ ), BJ ( $n = 10$ ), TY ( $n = 7$ ), and XA ( $n = 4$ ). This suggests that the abundance of aerosol



310 NACs in northern cities is indeed significantly contributed by biomass and coal  
 311 combustion. In most northern cities, the vehicle emission tracer  $C_5H_7O_6S^-$  (Blair et al.,  
 312 2017; Wang et al., 2021) showed insignificant positive correlation with NACs (**Figure**  
 313 **3a**).  $C_5H_7O_6S^-$  only exhibited a significant positive correlation with NGs (a minor  
 314 NACs component) in BJ. This suggests that the contribution of vehicle emissions to  
 315 aerosol NACs in northern cities may be significantly smaller than that of biomass and  
 316 coal combustion. In southern cities, the highest frequency of significant positive  
 317 correlations between NACs and biomass burning or coal combustion tracers was found  
 318 in KM ( $n = 22$ ), followed by CD ( $n = 19$ ), HZ ( $n = 15$ ), GY ( $n = 10$ ), WH ( $n = 10$ ), and  
 319 GZ ( $n = 5$ ) (**Figure 3b, c**). Clearly, the frequency of significant positive correlations  
 320 between NACs and biomass burning or coal combustion tracers was generally higher  
 321 in southern China than in northern China (**Figure 3**). Although this does not necessarily  
 322 indicate that biomass burning released more NACs in southern China, the result is fully  
 323 consistent with the spatial distribution pattern shown in open fire spot maps, where  
 324 southern China exhibited a higher density of fire spots compared to northern China  
 325 (**Figure S5**). The vehicle emission tracer  $C_5H_7O_6S^-$  showed insignificant positive  
 326 correlations with NACs in any southern cities (**Figure 3b**). Given that NACs in the  
 327 actual atmospheric environment are affected not only by primary emissions but also by  
 328 secondary formation and removal processes, insignificant or weak correlations between  
 329 various NACs and source-specific tracers do not necessarily indicate a lack of  
 330 substantial influence from corresponding sources. However, the above correlation  
 331 analysis can at least suggest that biomass and coal combustion play important roles in





controlling aerosol NAC abundances in both northern and southern Chinese cities.

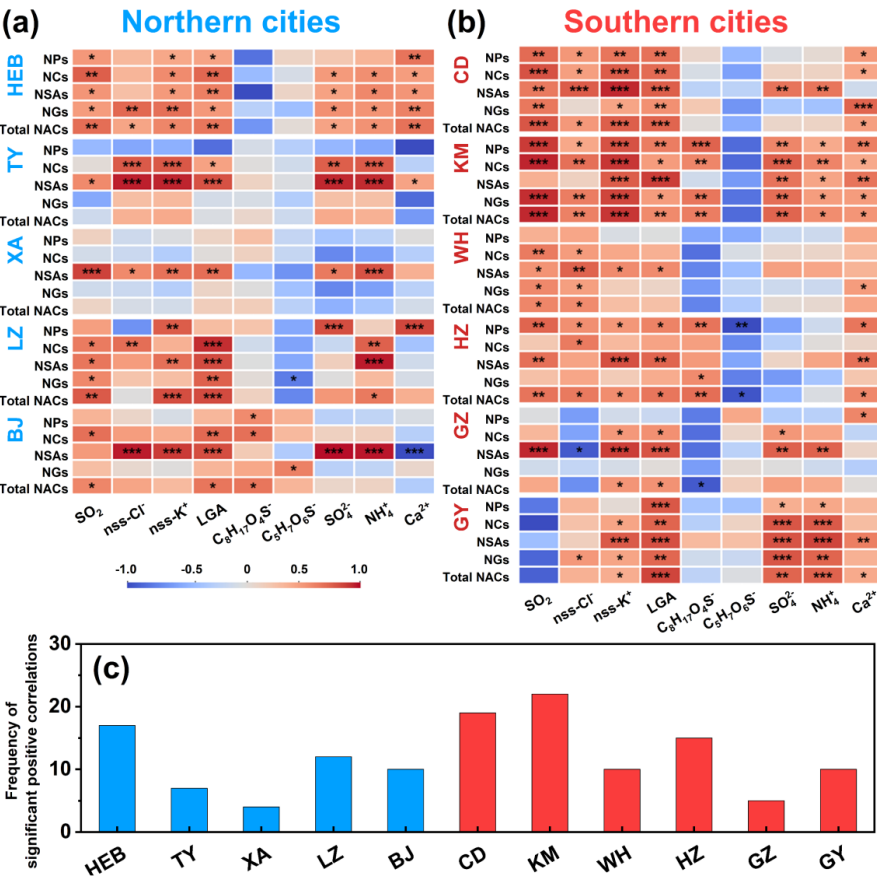


**Figure 3.** Correlations between various NAC species and indicative parameters in (a) northern and (b) southern China. The colors of different solid rectangles indicate different correlation coefficients  $r$ . Symbols \* and \*\* indicate  $P < 0.05$  and  $P < 0.01$ , respectively. NACs are categorized into four groups, including nitrophenols (NPs), nitrocatechols (NCs), nitrosalicylic acids (NSAs), and nitroguaiacols (NGs). (c) Frequency of significant positive correlations between NACs and biomass burning or coal combustion tracers (i.e., the number of orange-red rectangles marked with asterisks



342 in the panels a and b).

343

344 Furthermore, it is important to note that a critical distinction should be made  
 345 regarding the role of biomass and coal combustion in shaping aerosol NAC composition  
 346 and abundances. These combustion sources emit both primary NACs and volatile  
 347 precursors that facilitate secondary NAC formation through atmospheric reactions.  
 348 Thus, even though the correlation analysis mentioned above strongly implies biomass  
 349 and coal combustion (typically considered primary sources) as significant contributors  
 350 to NACs in winter aerosols in China, this evidence alone cannot attribute the NAC  
 351 burden predominantly to direct primary emissions. The significant contributions may  
 352 be also derived from efficient secondary formation processes initiated by the precursors  
 353 co-emitted from these combustion activities.

354

355

### 356 **3.3. Aerosol NACs dominated by secondary formation**

357 To further determine the relative contributions of secondary oxidation processes  
 358 and primary emissions to the measured aerosol NACs, an approach based on a tracer  
 359 species was employed (Salvador et al., 2021; Li et al., 2019). This method is similar to  
 360 the elemental carbon-tracer technique utilized for estimating secondary organic carbon.  
 361 Its specific application refers to the following equation 1 (Chen et al., 2022; Liu et al.,  
 362 2023b).

$$363 \quad [\text{NACs}]_{\text{sec.}} = [\text{NACs}]_{\text{total}} - \left( \frac{[\text{NACs}]}{[\text{Tracer}]} \right)_{\text{pri.}} \times [\text{Tracer}] \quad (1)$$



364 where  $[NACs]_{sec.}$ ,  $[NACs]_{total}$ , and  $[Tracer]$  correspond to the concentrations of  
 365 secondarily formed NACs, the total measured NACs, and the tracer, respectively.  
 366 Carbon monoxide (CO) served as the indicator for combustion sources. The term  
 367  $(\frac{[NACs]}{[Tracer]})_{pri.}$  represents the concentration ratio of NACs to CO. This ratio was derived by  
 368 fitting the lowest 15% of the observed  $(\frac{[NACs]}{[Tracer]})$  values, with the underlying assumption  
 369 that these data reflect periods dominated by primary emissions (Chen et al., 2022).

370 **Figure 4** and **Figure S6** show the contribution of secondarily formed NACs to the  
 371 total measured NAC mass in  $PM_{2.5}$  across 11 Chinese cities. In northern cities, the  
 372 proportion of secondary NACs in the particle phase was highest in XA (92 %), followed  
 373 by HEB (91 %), BJ (87 %), LZ (83 %), and TY (80 %) (**Figure 4a** and **Table S5**). On  
 374 average, the contribution of secondarily formed NACs to the total aerosol NAC mass  
 375 in the investigated northern cities was 87%, which is slightly lower than that observed  
 376 in the southern cities (93%) (**Figure 4b** and **Table S5**). Among the southern cities, the  
 377 maximum and minimum average secondary NAC contributions to total aerosol NACs  
 378 were observed in GZ (96 %) and GY (88 %), respectively. Overall, the secondary  
 379 formation pathway dominated the total NAC masses in  $PM_{2.5}$  during winter in Chinese  
 380 cities. Similarly, an observational study on the secondary formation of brown carbon  
 381 conducted in Chongming Island, Shanghai, also reported that the fraction of secondary  
 382 NACs in  $PM_{2.5}$  exceeded 80% during haze episodes, further corroborating the  
 383 significance of secondary production in shaping aerosol NAC pollution (Liu et al.,  
 384 2023b).

385

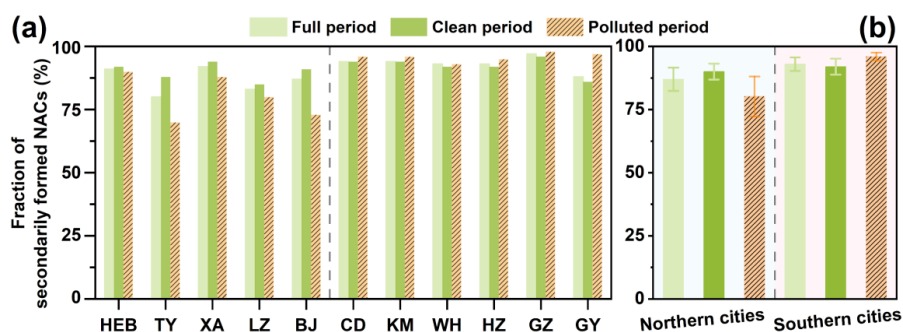


**Figure 4.** (a) Average contribution of secondarily formed NACs to the total measured NAC masses in  $PM_{2.5}$  in different periods across 11 Chinese cities. (b) Average contribution of secondarily formed NACs to the total measured NAC masses in  $PM_{2.5}$  in different periods in northern and southern China.

Furthermore, we observed a declining trend in the proportional contribution of secondarily formed NACs to total aerosol NACs from clean to polluted periods across all northern Chinese cities (**Figure 4**). This pattern suggests either an increased contribution from primary emission sources (e.g., biomass and coal combustion) to aerosol NACs, or the presence of limiting factors that suppress the yield of secondary NAC formation on polluted days. Biomass and coal combustion have been identified as significant primary sources of NACs during winter in China (**Figure 3**) (Salvador et al., 2021; Li et al., 2020a; Li et al., 2016); moreover, these anthropogenic activities occur regularly daily throughout the cold season. Thus, changing meteorological factors during polluted days (e.g., reduced planetary boundary layer height (PBLH) and weakened wind speed (**Tables S1–S4**)) may be important drivers of aerosol NAC accumulation. Nevertheless, the fact that the fraction of secondary NACs decreases



404 during northern pollution episodes implies the existence of specific factors that  
405 constrained secondary NAC yields under polluted conditions. In contrast, southern  
406 cities exhibit an increasing trend in the relative abundance of secondary NACs from  
407 clean to polluted periods. This pattern may be more intuitively explained, as elevated  
408 ALW concentrations, lower PBLH, and increased NO<sub>x</sub> levels during polluted episodes  
409 can promote the secondary formation of NACs or the direct partitioning of gaseous  
410 NACs into the particle phase. Overall, aerosol NACs in China during winter were  
411 dominated by secondary processes; however, the complex factors regulating NAC  
412 formation require further differentiation between northern and southern cities.

413

#### 414 **3.4. Potential promotion and constraint effects on the formation of aerosol NACs**

415 The secondary formation of NACs proceeds via gas-phase photochemical  
416 reactions and aqueous-phase processes within aerosols (Harrison et al., 2005; Yang et  
417 al., 2020). For example, the gas-phase process often begins with the oxidation of  
418 volatile aromatic precursors like benzene and toluene by ·OH, leading to the formation  
419 of phenolic compounds (Chen et al., 2022). These phenols can further react with ·OH  
420 during the day or with NO<sub>3</sub>· at night, generating phenoxy radicals (Wang and Li, 2021;  
421 Atkinson et al., 1992; Olariu et al., 2002; Olariu et al., 2013). The addition of NO<sub>2</sub> to  
422 these radicals results in the formation of nitrophenols and nitrocatechols (Rana and  
423 Guzman, 2022). Subsequently, these NACs can partition into the aqueous-phase in  
424 aerosols. Simultaneously, phenolic compounds in aqueous-phase can also undergo  
425 nitration (Vidović et al., 2018; Harrison et al., 2005). Thus, increased ALW levels are



426 expected to promote the enrichment of NACs in aerosol particles. Conversely,  
427 photodegradation and enhanced atmospheric oxidation capacity can facilitate the  
428 removal of NACs. Recent field observations and chamber experiments have suggested  
429 a significant positive correlation between the concentration of particulate NACs and  
430 RH (Xiong et al., 2025). The authors (Xiong et al., 2025) proposed a previously  
431 overlooked but efficient NAC formation pathway driven by gaseous water clusters, in  
432 addition to the well-known ALW mediated processes. Additionally, recent simulations  
433 on nitrate-mediated aqueous-phase photooxidation of NACs have suggested that  
434 increasing aerosol nitrate concentrations can significantly enhance the photolysis rates  
435 of 4-nitrocatechol, 3-nitrosalicylic acid, and 3,4-dinitrophenol by 3 to 3.5 times  
436 compared to nitrate-free cases (Liu et al., 2025). Consequently, we further examined  
437 the correlations between the abundance of NACs and the key factors affecting their  
438 formation (e.g., ALW, RH, radiation intensity, atmospheric oxidation capacity, and  
439 nitrate levels) in field environments (**Figure 5**). This approach is commonly employed  
440 in observation studies to identify the critical factors affecting the concentrations of  
441 target compounds (Yang et al., 2020; Liu et al., 2023b; Huang et al., 2023; Liu et al.,  
442 2023a; Gui et al., 2025).

443

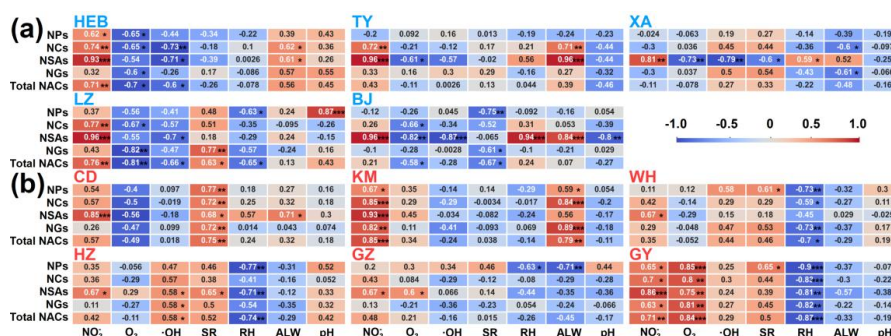


**Figure 5.** Correlations between various NAC species and factors potentially affecting their formation in (a) northern and (b) southern China. The colors of different solid rectangles indicate different correlation coefficients  $r$  (shown inside the rectangles). Symbols \* and \*\* indicate  $P < 0.05$  and  $P < 0.01$ , respectively.

In most northern Chinese cities (e.g., HEB, TY, XA, and LZ), insignificant positive correlations were observed between various NACs (except NSAs) and RH; instead, negative correlations were identified between them (**Figure 5a**). In XA and BJ, only NSAs show a significant positive correlation with RH. Similarly, a general negative correlation trend between NACs and RH was prevalent in southern cities (**Figure 5b**). These field observations clearly contrasted with recently reported laboratory findings where RH was shown to significantly promote NAC formation. This indicates that NAC formation in complex real-world environments may be co-controlled by multiple factors. The correlation patterns between ALW and NACs were largely similar to those of RH across most investigated Chinese cities. However, in TY and KM, ALW showed significant positive correlations with NACs. Furthermore, we found that ALW and RH levels were generally higher on polluted days compared to clean days across the studied



462 cities (**Figure S7** and **Tables S1–S4**). However, as discussed above, the concentrations  
 463 of major NAC species did not increase in some cities (**Figure 1**), further implying that  
 464 ALW and RH are not deterministic factors for NAC accumulation during pollution  
 465 episodes. Although a recent study conducted a laboratory located in XA has suggested  
 466 that increased aerosol nitrate can enhance NAC photolysis (Liu et al., 2025), nitrate  
 467 concentrations showed a positive correlation with NACs in most investigated cities  
 468 (except XA) (**Figure 5**). This suggests that in ambient environments, the significant  
 469 positive correlation between nitrate (a common transformation product of combustion-  
 470 derived  $\text{NO}_x$ ) and NACs likely indicates that NAC formation is closely linked to  
 471 combustion emissions and  $\text{NO}_x$ -involved secondary chemistry. In addition, atmospheric  
 472 oxidants (e.g.,  $\text{O}_3$  and  $\cdot\text{OH}$ ) and SR exhibited negative correlations with NACs in most  
 473 northern cities. In contrast,  $\text{O}_3$ ,  $\cdot\text{OH}$  and SR exerted a promoting effect on NAC  
 474 formation in some southern cities such as CD, WH, HZ, and GY. These distinctions  
 475 underscore the necessity for region-specific assessment of NAC formation mechanisms  
 476 and their drivers.

477 To visually compare the key factors influencing the formation of aerosol NACs in  
 478 northern and southern China, we pooled data from all cities in these two regions to  
 479 perform Mantel test analysis and principal component analysis (PCA) (**Figure 6**). In  
 480 both southern and northern China, only NSAs exhibited a significant correlation with  
 481 ALW (**Figure 6a,b**). This is likely because the carboxyl group present in NSAs  
 482 promotes ionization in water, thereby enhancing their solubility. Although PCA results  
 483 intuitively indicate the homology of various NACs (excluding NSAs) (**Figure 6c,d**),





484 the significant promotional effects of RH and ALW on NCs, NPs, and NGs were not  
485 reflected in either the Mantel test or PCA analyses. Furthermore, in northern Chins, SR  
486 was distributed in a nearly opposite direction to NCs, NPs, and NGs in the PCA plot  
487 (**Figure 6c**), suggesting an inhibitory role of photodegradation on their accumulation in  
488 particles (Liu et al., 2024). During winter, the atmospheric fine particulate pollution is  
489 generally more severe in northern cities than in southern cities (**Figure 1f** and **Tables**  
490 **S1–S4**), and the abundance of NACs is also greater in the north (**Figure 1f** and **Figure**  
491 **S3**). These findings imply that the light absorption capacity of aerosols in northern cities  
492 are stronger than in southern cities (Huang et al., 2024). This may explain why NACs  
493 in northern cities showed a significant negative correlation with SR and why the  
494 proportion of secondarily formed NACs in the total measured NACs was lower in the  
495 north than in the south, especially during pollution episodes. Additionally, the  
496 constraining effect of  $O_3$  or  $\cdot OH$  on NAC formation was greater in northern China  
497 (evidenced by larger angles between them in **Figure 6c**) than in southern China (**Figure**  
498 **6d**). Similar conclusions can also be more intuitively obtained in the Mantel test  
499 analysis results (**Figure 6a,b**). Overall, our findings indicate that the promotional  
500 effects of RH and ALW on NAC formation were insignificant in field observation in  
501 China during winter. This could be attributed to the synergistic constraints of multiple  
502 factors, such as photolysis,  $O_3$ , and  $\cdot OH$  (**Figure 7**).

503

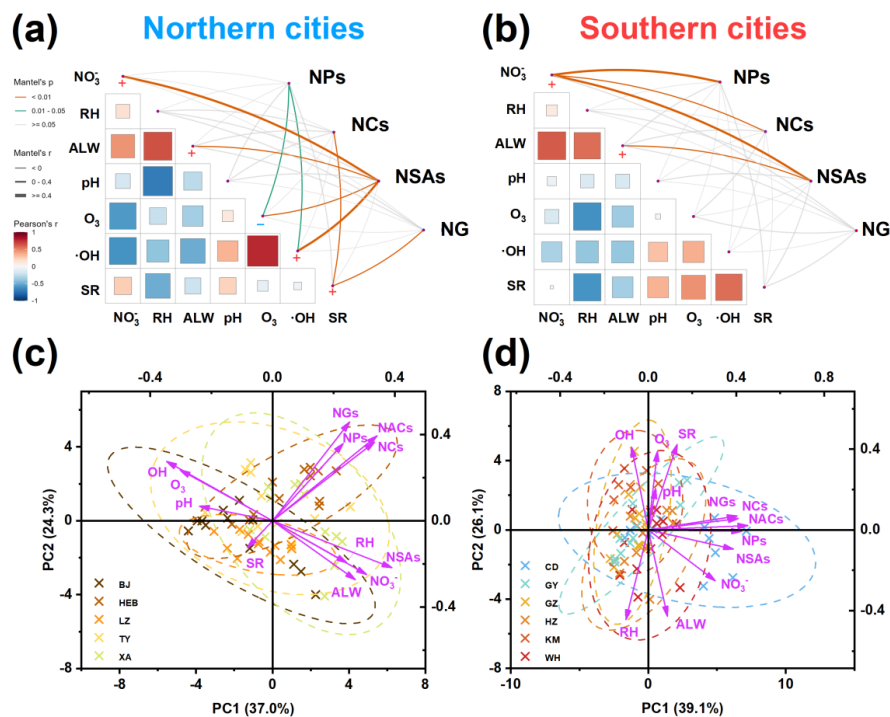


**Figure 6.** Mantel test correlation heatmap showing the interrelationships between different factors or parameters for the pooled data from (a) northern and (b) southern China. The size of the solid square indicates the significance of the correlation between the two corresponding parameters. The larger square indicates that the correlation is more significant. The colors of the different solid circles indicate different correlation coefficients ( $r$ ). The symbols ‘+’ and ‘-’ refer to positive and negative correlations, respectively. Principal component analysis result deciphering the interrelationships among different factors or parameters for the pooled data from (c) northern and (d) southern China.

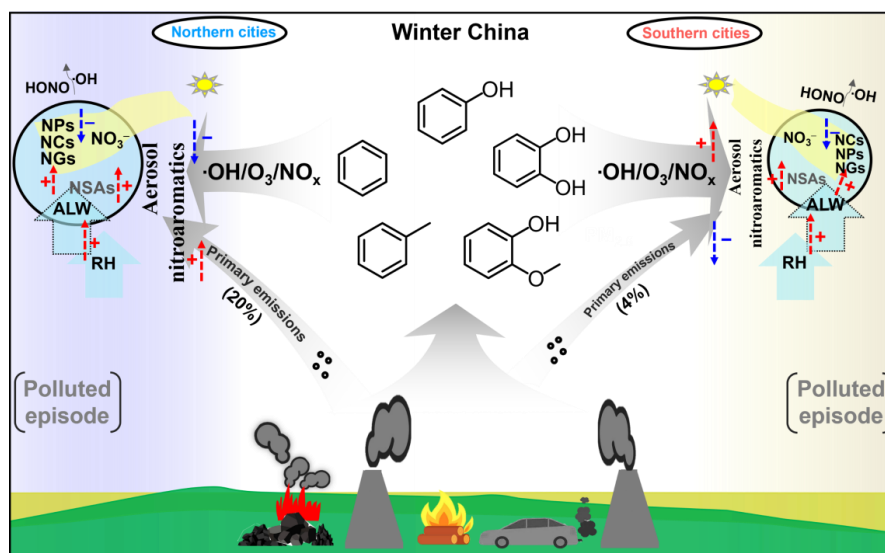


**Figure 7.** Conceptual illustration showing that the secondary processes driven by multi-factor interactions modulate the aerosol NAC pollution during winter in southern and northern China. The “+” and “-” symbols indicate promoting and constraining effects, respectively.

#### 4. Conclusion and atmospheric implications

To the best of our knowledge, this study presents the first simultaneous investigation of the abundance, composition, and origins of NACs in  $PM_{2.5}$  across 11 Chinese cities during winter, along with the key factors controlling their formation. On average, NPs and NCs were identified as the two predominant groups of NACs. Their relative contributions to the total NAC abundance varied by city, with either NPs or NCs being dominant depending on location. Overall, the abundance of aerosol NACs was higher in northern China compared to southern China, likely attributable to more intensive coal and biomass burning activities in the north. Furthermore, we found that



530 aerosol NACs in China during winter were predominantly formed via secondary  
531 processes. However, the proportion of secondarily formed NACs in the total measured  
532 NACs was lower in the north than in the south. This north-south difference was further  
533 amplified during polluted periods.

534       The significant promotional effects of RH and ALW on NCs, NPs, and NGs were  
535 not observed in either northern or southern China. Only NSAs showed a significant  
536 positive correlation with ALW across both regions. Furthermore, the constraining  
537 effects of O<sub>3</sub>, ·OH, or SR on NAC formation were more pronounced in northern China  
538 compared to southern China. This may have attenuated the promotional effects of RH  
539 and ALW on NAC formation (**Figure 7**). Previous observational and simulation studies  
540 have emphasized the significant promotional role of RH and ALW in the formation of  
541 aerosol nitrogen-containing organic compounds (including NACs) (Xiong et al., 2025;  
542 Xu et al., 2020b; Ma et al., 2025). However, this large-scale observational study  
543 suggests that the generalizability of such RH- and ALW-regulated promotional effects  
544 on NAC formation in real atmospheric environments requires further validation. We  
545 acknowledge that individual factors (e.g., RH or ALW) play a crucial role in governing  
546 aerosol NAC formation. Nevertheless, field environments are often more complex than  
547 laboratory-simulated scenarios. Thus, the overall results highlight that future  
548 investigations into NAC formation mechanisms should consider the impacts of multi-  
549 factor interactions.

550

551 **Data availability.** The data presented in this work are available upon request from the



552 corresponding authors.

553

554 **Author contributions.** YX, HYX, and HX designed the study; YX, YCY, TY, LG, JLT,  
555 TSC, HWX, and HX performed field measurements and sample collection; TY and  
556 YCY performed chemical analysis; YX and YCY performed data analysis; YX wrote  
557 the original manuscript; HYX and HX provided suggestions, and YX reviewed and  
558 edited the manuscript.

559

560 **Financial support.** This study was kindly supported by Key Program of the National  
561 Natural Science Foundation of China (grant number 42430501), National Natural  
562 Science Foundation of China (grant number 42303081 and 42403077), National Key  
563 Research and Development Program of China (grant number 2023YFF0806001).

564

565 **Conflict of Interest.** The authors declare no conflicts of interest relevant to this study.

566

567



## 568 **References**

- 569       Atkinson, R., Aschmann, S. M., and Arey, J.: Reactions of hydroxyl and nitrogen  
 570       trioxide radicals with phenol, cresols, and 2-nitrophenol at 296  $\pm$  2 K, Environmental  
 571       Science & Technology, 26, 1397-1403, 10.1021/es00031a018, 1992.
- 572       Blair, S. L., MacMillan, A. C., Drozd, G. T., Goldstein, A. H., Chu, R. K., Paša-  
 573       Tolić, L., Shaw, J. B., Tolić, N., Lin, P., Laskin, J., Laskin, A., and Nizkorodov, S. A.:  
 574       Molecular Characterization of Organosulfur Compounds in Biodiesel and Diesel Fuel  
 575       Secondary Organic Aerosol, Environmental Science & Technology, 51, 119-127,  
 576       10.1021/acs.est.6b03304, 2017.
- 577       Boreddy, S. K. R. and Kawamura, K.: A 12-year observation of water-soluble ions  
 578       in TSP aerosols collected at a remote marine location in the western North Pacific: an  
 579       outflow region of Asian dust, Atmos. Chem. Phys., 15, 6437-6453, 10.5194/acp-15-  
 580       6437-2015, 2015.
- 581       Cai, D., Wang, X., George, C., Cheng, T., Herrmann, H., Li, X., and Chen, J.:  
 582       Formation of Secondary Nitroaromatic Compounds in Polluted Urban Environments,  
 583       Journal of Geophysical Research: Atmospheres, 127, e2021JD036167,  
 584       https://doi.org/10.1029/2021JD036167, 2022.
- 585       Chen, Y., Zheng, P., Wang, Z., Pu, W., Tan, Y., Yu, C., Xia, M., Wang, W., Guo, J.,  
 586       Huang, D., Yan, C., Nie, W., Ling, Z., Chen, Q., Lee, S., and Wang, T.: Secondary  
 587       Formation and Impacts of Gaseous Nitro-Phenolic Compounds in the Continental  
 588       Outflow Observed at a Background Site in South China, Environmental Science &  
 589       Technology, 56, 6933-6943, 10.1021/acs.est.1c04596, 2022.



590 Ehhalt, D. H. and Rohrer, F.: Dependence of the OH concentration on solar UV, J.  
591 Geophys. Res.: Atmos., 105, 3565-3571, 10.1029/1999jd901070, 2000.

592 Finewax, Z., de Gouw, J. A., and Ziemann, P. J.: Identification and Quantification  
593 of 4-Nitrocatechol Formed from OH and NO<sub>3</sub> Radical-Initiated Reactions of Catechol  
594 in Air in the Presence of NO<sub>x</sub>: Implications for Secondary Organic Aerosol Formation  
595 from Biomass Burning, Environmental Science & Technology, 52, 1981-1989,  
596 10.1021/acs.est.7b05864, 2018.

597 Frka, S., Šala, M., Brodnik, H., Štefane, B., Kroflič, A., and Grgić, I.: Seasonal  
598 variability of nitroaromatic compounds in ambient aerosols: Mass size distribution,  
599 possible sources and contribution to water-soluble brown carbon light absorption,  
600 Chemosphere, 299, 134381, <https://doi.org/10.1016/j.chemosphere.2022.134381>, 2022.

601 Gu, C., Cui, S., Ge, X., Wang, Z., Chen, M., Qian, Z., Liu, Z., Wang, X., and Zhang,  
602 Y.: Chemical composition, sources and optical properties of nitrated aromatic  
603 compounds in fine particulate matter during winter foggy days in Nanjing, China,  
604 Environmental Research, 212, 113255, <https://doi.org/10.1016/j.envres.2022.113255>,  
605 2022.

606 Gui, L., Xu, Y., Ma, Y.-J., Yang, T., Xiao, H.-W., Xiao, H., and Xiao, H.-Y.:  
607 Firework Display Is a Newly Identified Source of Gaseous and Particulate Amines,  
608 Environmental Science & Technology Letters, 12, 1387-1393,  
609 10.1021/acs.estlett.5c00806, 2025.

610 Gui, L., Xu, Y., You, Y.-C., Ma, Y.-J., Yang, T., Liu, T., Xiao, H.-W., Xiao, H., and  
611 Xiao, H.-Y.: Oxidative Degradation of Higher-Molecular-Weight Aromatic Amine



612 Compounds Is a Potential Source of Anilinium in Urban Aerosols, Environ. Sci.  
 613 Technol. Lett., 11, 1355–1361, 10.1021/acs.estlett.4c00935, 2024.

614 Guo, Z., Hu, X., Sun, W., Peng, X., Fu, Y., Liu, K., Liu, F., Meng, H., Zhu, Y.,  
 615 Zhang, G., Wang, X., Xue, L., Wang, J., Wang, X., Peng, P. a., and Bi, X.: Mixing state  
 616 and influence factors controlling diurnal variation of particulate nitrophenol  
 617 compounds at a suburban area in northern China, Environmental pollution, 344, 123368,  
 618 <https://doi.org/10.1016/j.envpol.2024.123368>, 2024.

619 Hao, Y., Sun, G., Fan, T., Tang, X., Zhang, J., Liu, Y., Zhang, N., Zhao, L., Zhong,  
 620 R., and Peng, Y.: In vivo toxicity of nitroaromatic compounds to rats: QSTR modelling  
 621 and interspecies toxicity relationship with mouse, Journal of Hazardous Materials, 399,  
 622 122981, <https://doi.org/10.1016/j.jhazmat.2020.122981>, 2020.

623 Harrison, M. A. J., Barra, S., Borghesi, D., Vione, D., Arsene, C., and Iulian Olariu,  
 624 R.: Nitrated phenols in the atmosphere: a review, Atmospheric Environment, 39, 231-  
 625 248, <https://doi.org/10.1016/j.atmosenv.2004.09.044>, 2005.

626 Huang, S., Shen, Z., Bai, G., Zhang, L., Wang, D., Li, C., Zheng, H., Xu, H., and  
 627 Zhang, Y.: Photochemical Aging of PM<sub>2.5</sub> Nitroaromatic Compounds From Solid Fuel  
 628 Combustion Enhanced Light Absorption and Oxidation Potential, Journal of  
 629 Geophysical Research: Atmospheres, 130, e2025JD043471,  
 630 <https://doi.org/10.1029/2025JD043471>, 2025.

631 Huang, S., Yang, X., Xu, H., Zeng, Y., Li, D., Sun, J., Ho, S. S. H., Zhang, Y., Cao,  
 632 J., and Shen, Z.: Insights into the nitroaromatic compounds, formation, and light  
 633 absorption contributing emissions from various geological maturity coals, Science of





634 The Total Environment, 870, 162033, <https://doi.org/10.1016/j.scitotenv.2023.162033>,  
635 2023.

636 Huang, S., Shen, Z., Yang, X., Bai, G., Zhang, L., Zeng, Y., Sun, J., Xu, H., Ho, S.  
637 S. H., Zhang, Y., and Cao, J.: Nitroaromatic compounds in six major Chinese cities:  
638 Influence of different formation mechanisms on light absorption properties, Science of  
639 The Total Environment, 930, 172672, <https://doi.org/10.1016/j.scitotenv.2024.172672>,  
640 2024.

641 Huo, Y., Li, M., Wang, X., Sun, J., Zhou, Y., Ma, Y., and He, M.: Rapid oxidation  
642 of phenolic compounds by O<sub>3</sub> and HO●: effects of the air–water interface and mineral  
643 dust in tropospheric chemical processes, Atmos. Chem. Phys., 24, 12409-12423,  
644 [10.5194/acp-24-12409-2024](https://doi.org/10.5194/acp-24-12409-2024), 2024.

645 Kahnt, A., Behrouzi, S., Vermeylen, R., Safi Shalamzari, M., Vercauteren, J.,  
646 Roekens, E., Claeys, M., and Maenhaut, W.: One-year study of nitro-organic  
647 compounds and their relation to wood burning in PM<sub>10</sub> aerosol from a rural site in  
648 Belgium, Atmospheric Environment, 81, 561-568,  
649 <https://doi.org/10.1016/j.atmosenv.2013.09.041>, 2013.

650 Kroflič, A., Anders, J., Drventić, I., Mettke, P., Böge, O., Mutzel, A., Kleffmann,  
651 J., and Herrmann, H.: Guaiacol Nitration in a Simulated Atmospheric Aerosol with an  
652 Emphasis on Atmospheric Nitrophenol Formation Mechanisms, ACS Earth and Space  
653 Chemistry, 5, 1083-1093, [10.1021/acsearthspacechem.1c00014](https://doi.org/10.1021/acsearthspacechem.1c00014), 2021.

654 Li, K., Li, J., Tong, S., Wang, W., Huang, R. J., and Ge, M.: Characteristics of  
655 wintertime VOCs in suburban and urban Beijing: concentrations, emission ratios, and



656 festival effects, *Atmos. Chem. Phys.*, 19, 8021-8036, 10.5194/acp-19-8021-2019, 2019.

657 Li, M., Wang, X., Lu, C., Li, R., Zhang, J., Dong, S., Yang, L., Xue, L., Chen, J.,

658 and Wang, W.: Nitrated phenols and the phenolic precursors in the atmosphere in urban

659 Jinan, China, *Science of The Total Environment*, 714, 136760,

660 <https://doi.org/10.1016/j.scitotenv.2020.136760>, 2020a.

661 Li, X., Yang, Y., Liu, S., Zhao, Q., Wang, G., and Wang, Y.: Light absorption

662 properties of brown carbon (BrC) in autumn and winter in Beijing: Composition,

663 formation and contribution of nitrated aromatic compounds, *Atmospheric Environment*,

664 223, 117289, <https://doi.org/10.1016/j.atmosenv.2020.117289>, 2020b.

665 Li, X., Wang, Y., Hu, M., Tan, T., Li, M., Wu, Z., Chen, S., and Tang, X.:

666 Characterizing chemical composition and light absorption of nitroaromatic compounds

667 in the winter of Beijing, *Atmospheric Environment*, 237, 117712,

668 <https://doi.org/10.1016/j.atmosenv.2020.117712>, 2020c.

669 Li, X., Jiang, L., Hoa, L. P., Lyu, Y., Xu, T., Yang, X., Iinuma, Y., Chen, J., and

670 Herrmann, H.: Size distribution of particle-phase sugar and nitrophenol tracers during

671 severe urban haze episodes in Shanghai, *Atmospheric Environment*, 145, 115-127,

672 <https://doi.org/10.1016/j.atmosenv.2016.09.030>, 2016.

673 Liao, T., Wang, S., Ai, J., Gui, K., Duan, B., Zhao, Q., Zhang, X., Jiang, W., and

674 Sun, Y.: Heavy pollution episodes, transport pathways and potential sources of PM<sub>2.5</sub>

675 during the winter of 2013 in Chengdu (China), *Science of The Total Environment*, 584-

676 585, 1056-1065, <https://doi.org/10.1016/j.scitotenv.2017.01.160>, 2017.

677 Liu, S., Wang, H., Hu, Z., Zhang, X., Sun, Y., and Dong, F.: Resolving the



678 overlooked photochemical nitrophenol transformation mechanism induced by  
 679 nonradical species under visible light, *Proceedings of the National Academy of*  
 680 *Sciences*, 121, e2401452121, doi:10.1073/pnas.2401452121, 2024.

681 Liu, T., Xu, Y., Sun, Q.-B., Xiao, H.-W., Zhu, R.-G., Li, C.-X., Li, Z.-Y., Zhang,  
 682 K.-Q., Sun, C.-X., and Xiao, H.-Y.: Characteristics, Origins, and Atmospheric  
 683 Processes of Amines in Fine Aerosol Particles in Winter in China, *J. Geophys. Res.:*  
 684 *Atmos.*, 128, e2023JD038974, <https://doi.org/10.1029/2023JD038974>, 2023a.

685 Liu, X., Wang, H., Wang, F., Lv, S., Wu, C., Zhao, Y., Zhang, S., Liu, S., Xu, X.,  
 686 Lei, Y., and Wang, G.: Secondary Formation of Atmospheric Brown Carbon in China  
 687 Haze: Implication for an Enhancing Role of Ammonia, *Environmental Science &*  
 688 *Technology*, 57, 11163-11172, 10.1021/acs.est.3c03948, 2023b.

689 Liu, Y., Huang, R.-J., Lin, C., Yuan, W., Li, Y. J., Zhong, H., Yang, L., Wang, T.,  
 690 Huang, W., Xu, W., Huang, D. D., and Huang, C.: Nitrate-Photolysis Shortens the  
 691 Lifetimes of Brown Carbon Tracers from Biomass Burning, *Environmental Science &*  
 692 *Technology*, 59, 640-649, 10.1021/acs.est.4c06123, 2025.

693 Lu, C., Wang, X., Dong, S., Zhang, J., Li, J., Zhao, Y., Liang, Y., Xue, L., Xie, H.,  
 694 Zhang, Q., and Wang, W.: Emissions of fine particulate nitrated phenols from various  
 695 on-road vehicles in China, *Environmental Research*, 179, 108709,  
 696 <https://doi.org/10.1016/j.envres.2019.108709>, 2019.

697 Ma, Y. J., Xu, Y., Yang, T., Xiao, H. W., and Xiao, H. Y.: Measurement report:  
 698 Characteristics of nitrogen-containing organics in PM<sub>2.5</sub> in Ürümqi, northwestern  
 699 China – differential impacts of combustion of fresh and aged biomass materials, *Atmos.*



700 Chem. Phys., 24, 4331-4346, 10.5194/acp-24-4331-2024, 2024.

701 Ma, Y. J., Xu, Y., Yang, T., Gui, L., Xiao, H. W., Xiao, H., and Xiao, H. Y.: The  
702 critical role of aqueous-phase processes in aromatic-derived nitrogen-containing  
703 organic aerosol formation in cities with different energy consumption patterns, Atmos.  
704 Chem. Phys., 25, 2763-2780, 10.5194/acp-25-2763-2025, 2025.

705 MacFarlane, S. M., Fisher, J. A., Xu, L., Wennberg, P. O., Crounse, J. D., Ball, K.,  
706 Zhai, S., Bates, K. H., Kim, Y., Zhang, Q., and Blake, D. R.: Sources, Sinks, and  
707 Oxidation Pathways of Phenolic Compounds in South Korea Constrained Using  
708 KORUS-AQ Airborne Observations, Journal of Geophysical Research: Atmospheres,  
709 130, e2024JD043110, <https://doi.org/10.1029/2024JD043110>, 2025.

710 Mayorga, R. J., Zhao, Z., and Zhang, H.: Formation of secondary organic aerosol  
711 from nitrate radical oxidation of phenolic VOCs: Implications for nitration mechanisms  
712 and brown carbon formation, Atmospheric Environment, 244, 117910,  
713 <https://doi.org/10.1016/j.atmosenv.2020.117910>, 2021.

714 Mohr, C., Lopez-Hilfiker, F. D., Zotter, P., Prévôt, A. S. H., Xu, L., Ng, N. L.,  
715 Herndon, S. C., Williams, L. R., Franklin, J. P., Zahniser, M. S., Worsnop, D. R.,  
716 Knighton, W. B., Aiken, A. C., Gorkowski, K. J., Dubey, M. K., Allan, J. D., and  
717 Thornton, J. A.: Contribution of Nitrated Phenols to Wood Burning Brown Carbon  
718 Light Absorption in Detling, United Kingdom during Winter Time, Environmental  
719 Science & Technology, 47, 6316-6324, 10.1021/es400683v, 2013.

720 Morales, J. A., Pirela, D., de Nava, M. G., de Borrego, B. z. S., Velásquez, H., and  
721 Durán, J.: Inorganic water soluble ions in atmospheric particles over Maracaibo Lake



- 722 Basin in the western region of Venezuela, *Atmospheric Research*, 46, 307-320,  
723 [https://doi.org/10.1016/S0169-8095\(97\)00071-9](https://doi.org/10.1016/S0169-8095(97)00071-9), 1998.
- 724 Nguyen, T. K. V., Zhang, Q., Jimenez, J. L., Pike, M., and Carlton, A. G.: Liquid  
725 water: ubiquitous contributor to aerosol mass, *Environ. Sci. Tech. Lett.*, 3, 257-263.  
726 <https://doi.org/210.1021/acs.estlett.1026b00167>, 2016.
- 727 Olariu, R. I., Klotz, B., Barnes, I., Becker, K. H., and Mocanu, R.: FT–IR study of  
728 the ring-retaining products from the reaction of OH radicals with phenol, o-, m-, and p-  
729 cresol, *Atmospheric Environment*, 36, 3685-3697, [https://doi.org/10.1016/S1352-](https://doi.org/10.1016/S1352-2310(02)00202-9)  
730 [2310\(02\)00202-9](https://doi.org/10.1016/S1352-2310(02)00202-9), 2002.
- 731 Olariu, R. I., Barnes, I., Bejan, I., Arsene, C., Vione, D., Klotz, B., and Becker, K.  
732 H.: FT-IR Product Study of the Reactions of NO<sub>3</sub> Radicals With ortho-, meta-, and  
733 para-Cresol, *Environmental Science & Technology*, 47, 7729-7738,  
734 [10.1021/es401096w](https://doi.org/10.1021/es401096w), 2013.
- 735 Rana, M. S. and Guzman, M. I.: Oxidation of Catechols at the Air–Water Interface  
736 by Nitrate Radicals, *Environmental Science & Technology*, 56, 15437-15448,  
737 [10.1021/acs.est.2c05640](https://doi.org/10.1021/acs.est.2c05640), 2022.
- 738 Salvador, C. M. G., Tang, R., Priestley, M., Li, L., Tsiligiannis, E., Le Breton, M.,  
739 Zhu, W., Zeng, L., Wang, H., Yu, Y., Hu, M., Guo, S., and Hallquist, M.: Ambient nitro-  
740 aromatic compounds – biomass burning versus secondary formation in rural China,  
741 *Atmos. Chem. Phys.*, 21, 1389-1406, [10.5194/acp-21-1389-2021](https://doi.org/10.5194/acp-21-1389-2021), 2021.
- 742 Sareen, N., Waxman, E. M., Turpin, B. J., Volkamer, R., and Carlton, A. G.:  
743 Potential of aerosol liquid water to facilitate organic aerosol formation: assessing



744 knowledge gaps about precursors and partitioning, *Environ. Sci. Technol.*, 51, 3327-  
745 3335, 2017.

746 Selimovic, V., Yokelson, R. J., McMeeking, G. R., and Coefield, S.: Aerosol Mass  
747 and Optical Properties, Smoke Influence on O<sub>3</sub>, and High NO<sub>3</sub> Production Rates in a  
748 Western U.S. City Impacted by Wildfires, *Journal of Geophysical Research:*  
749 *Atmospheres*, 125, e2020JD032791, <https://doi.org/10.1029/2020JD032791>, 2020.

750 Shi, X., Qiu, X., Li, A., Jiang, X., Wei, G., Zheng, Y., Chen, Q., Chen, S., Hu, M.,  
751 Rudich, Y., and Zhu, T.: Polar Nitrated Aromatic Compounds in Urban Fine Particulate  
752 Matter: A Focus on Formation via an Aqueous-Phase Radical Mechanism,  
753 *Environmental Science & Technology*, 57, 5160-5168, 10.1021/acs.est.2c07324, 2023.

754 Vidović, K., Kroflič, A., Jovanović, P., Šala, M., and Grgić, I.: Electrochemistry  
755 as a Tool for Studies of Complex Reaction Mechanisms: The Case of the Atmospheric  
756 Aqueous-Phase Aging of Catechols, *Environmental Science & Technology*, 53, 11195-  
757 11203, 10.1021/acs.est.9b02456, 2019.

758 Vidović, K., Lašić Jurković, D., Šala, M., Kroflič, A., and Grgić, I.: Nighttime  
759 Aqueous-Phase Formation of Nitrocatechols in the Atmospheric Condensed Phase,  
760 *Environmental Science & Technology*, 52, 9722-9730, 10.1021/acs.est.8b01161, 2018.

761 Wang, D., Shen, Z., Zhang, Q., Lei, Y., Zhang, T., Huang, S., Sun, J., Xu, H., and  
762 Cao, J.: Winter brown carbon over six of China's megacities: light absorption,  
763 molecular characterization, and improved source apportionment revealed by multilayer  
764 perceptron neural network, *Atmos. Chem. Phys.*, 22, 14893-14904, 10.5194/acp-22-  
765 14893-2022, 2022.



- 766 Wang, H., Gao, Y., Wang, S., Wu, X., Liu, Y., Li, X., Huang, D., Lou, S., Wu, Z.,  
 767 Guo, S., Jing, S., Li, Y., Huang, C., Tyndall, G. S., Orlando, J. J., and Zhang, X.:  
 768 Atmospheric Processing of Nitrophenols and Nitrocresols From Biomass Burning  
 769 Emissions, *Journal of Geophysical Research: Atmospheres*, 125, e2020JD033401,  
 770 <https://doi.org/10.1029/2020JD033401>, 2020.
- 771 Wang, S. and Li, H.: NO<sub>3</sub><sup>·</sup>-Initiated Gas-Phase Formation of Nitrated Phenolic  
 772 Compounds in Polluted Atmosphere, *Environmental Science & Technology*, 55, 2899-  
 773 2907, 10.1021/acs.est.0c08041, 2021.
- 774 Wang, X., Gu, R., Wang, L., Xu, W., Zhang, Y., Chen, B., Li, W., Xue, L., Chen,  
 775 J., and Wang, W.: Emissions of fine particulate nitrated phenols from the burning of  
 776 five common types of biomass, *Environmental pollution*, 230, 405-412,  
 777 <https://doi.org/10.1016/j.envpol.2017.06.072>, 2017.
- 778 Wang, Y., Zhao, Y., Wang, Y., Yu, J. Z., Shao, J., Liu, P., Zhu, W., Cheng, Z., Li,  
 779 Z., Yan, N., and Xiao, H.: Organosulfates in atmospheric aerosols in Shanghai, China:  
 780 seasonal and interannual variability, origin, and formation mechanisms, *Atmos. Chem.*  
 781 *Phys.*, 21, 2959-2980, 10.5194/acp-21-2959-2021, 2021.
- 782 Wang, Y., Hu, M., Wang, Y., Zheng, J., Shang, D., Yang, Y., Liu, Y., Li, X., Tang,  
 783 R., Zhu, W., Du, Z., Wu, Y., Guo, S., Wu, Z., Lou, S., Hallquist, M., and Yu, J. Z.: The  
 784 formation of nitro-aromatic compounds under high NO<sub>x</sub> and anthropogenic VOC  
 785 conditions in urban Beijing, China, *Atmos. Chem. Phys.*, 19, 7649-7665, 10.5194/acp-  
 786 19-7649-2019, 2019.
- 787 Xie, M., Chen, X., Hays, M. D., and Holder, A. L.: Composition and light



788 absorption of N-containing aromatic compounds in organic aerosols from laboratory  
 789 biomass burning, *Atmos. Chem. Phys.*, 19, 2899-2915, 10.5194/acp-19-2899-2019,  
 790 2019.

791 Xiong, H., Liu, X., Sun, C., Zhang, X., Wang, X., Lin, J., Xue, L., Sun, X., Shang,  
 792 X., Ma, F., Xie, H., Chen, J., Yan, G., Shu, J., Fu, H., Wang, L., Rudich, Y., George, C.,  
 793 Mellouki, A., Zhao, D., Wang, X., Herrmann, H., and Chen, J.: Atmospheric water  
 794 cluster-catalyzed formation of nitroaromatics as a secondary aerosol source, *Science*  
 795 *Advances*, 11, eadv7805, doi:10.1126/sciadv.adv7805, 2025.

796 Xu, Y., Xiao, H., Wu, D., and Long, C.: Abiotic and Biological Degradation of  
 797 Atmospheric Proteinaceous Matter Can Contribute Significantly to Dissolved Amino  
 798 Acids in Wet Deposition, *Environ. Sci. Technol.*, 54, 6551-6561.  
 799 <https://doi.org/6510.1021/acs.est.6550c00421>, 2020a.

800 Xu, Y., Dong, X.-N., Xiao, H.-Y., Zhou, J.-X., and Wu, D.-S.: Proteinaceous  
 801 Matter and Liquid Water in Fine Aerosols in Nanchang, Eastern China: Seasonal  
 802 Variations, Sources, and Potential Connections, *J. Geophys. Res.: Atmos.*, 127,  
 803 e2022JD036589. <https://doi.org/036510.031029/032022JD036589>, 2022.

804 Xu, Y., Dong, X. N., He, C., Wu, D. S., Xiao, H. W., and Xiao, H. Y.: Mist cannon  
 805 trucks can exacerbate the formation of water-soluble organic aerosol and PM<sub>2.5</sub>  
 806 pollution in the road environment, *Atmos. Chem. Phys.*, 23, 6775-6788, 10.5194/acp-  
 807 23-6775-2023, 2023.

808 Xu, Y., Lin, X., Sun, Q.-B., Xiao, H.-W., Xiao, H., and Xiao, H.-Y.: Elaborating  
 809 the Atmospheric Transformation of Combined and Free Amino Acids From the





810 Perspective of Observational Studies, *J. Geophys. Res.: Atmos.*, 129, e2024JD040730.  
 811 <https://doi.org/040710.041029/042024JD040730>,  
 812 <https://doi.org/10.1029/2024JD040730>, 2024a.

813 Xu, Y., Liu, T., Ma, Y. J., Sun, Q. B., Xiao, H. W., Xiao, H., Xiao, H. Y., and Liu,  
 814 C. Q.: Measurement report: Occurrence of aminiums in PM<sub>2.5</sub> during winter in China  
 815 – aminium outbreak during polluted episodes and potential constraints, *Atmos. Chem.*  
 816 *Phys.*, 24, 10531-10542, 10.5194/acp-24-10531-2024, 2024b.

817 Xu, Y., Ma, Y. J., Yang, T., Sun, Q. B., Wang, Y. C., Gui, L., Xiao, H. W., Xiao, H.,  
 818 and Xiao, H. Y.: Molecular evidence on potential contribution of marine emissions to  
 819 aromatic and aliphatic organic sulfur and nitrogen aerosols in the South China Sea,  
 820 *Atmos. Chem. Phys.*, 25, 13621-13634, 10.5194/acp-25-13621-2025, 2025.

821 Xu, Y., Miyazaki, Y., Tachibana, E., Sato, K., Ramasamy, S., Mochizuki, T.,  
 822 Sadanaga, Y., Nakashima, Y., Sakamoto, Y., Matsuda, K., and Kajii, Y.: Aerosol Liquid  
 823 Water Promotes the Formation of Water-Soluble Organic Nitrogen in Submicrometer  
 824 Aerosols in a Suburban Forest, *Environ. Sci. Technol.*, 54, 1406-1414.  
 825 <https://doi.org/1410.1021/acs.est.1409b05849>, 2020b.

826 Yang, T., Xu, Y., Wang, Y. C., Ma, Y. J., Xiao, H. W., Xiao, H., and Xiao, H. Y.:  
 827 Non-biogenic sources are an important but overlooked contributor to aerosol isoprene-  
 828 derived organosulfates during winter in northern China, *Atmos. Chem. Phys.*, 25, 2967-  
 829 2978, 10.5194/acp-25-2967-2025, 2025.

830 Yang, T., Xu, Y., Ma, Y.-J., Wang, Y.-C., Yu, J. Z., Sun, Q.-B., Xiao, H.-W., Xiao,  
 831 H.-Y., and Liu, C.-Q.: Field Evidence for Constraints of Nearly Dry and Weakly Acidic



- 832 Aerosol Conditions on the Formation of Organosulfates, *Environ. Sci. Technol. Lett.*,  
833 11, 981-987, 10.1021/acs.estlett.4c00522, 2024.
- 834 Yang, T., Xu, Y., Ye, Q., Ma, Y. J., Wang, Y. C., Yu, J. Z., Duan, Y. S., Li, C. X.,  
835 Xiao, H. W., Li, Z. Y., Zhao, Y., and Xiao, H. Y.: Spatial and diurnal variations of aerosol  
836 organosulfates in summertime Shanghai, China: potential influence of photochemical  
837 processes and anthropogenic sulfate pollution, *Atmos. Chem. Phys.*, 23, 13433-13450,  
838 10.5194/acp-23-13433-2023, 2023.
- 839 Yang, W., You, D., Li, C., Han, C., Tang, N., Yang, H., and Xue, X.: Photolysis of  
840 Nitroaromatic Compounds under Sunlight: A Possible Daytime Photochemical Source  
841 of Nitrous Acid?, *Environmental Science & Technology Letters*, 8, 747-752,  
842 10.1021/acs.estlett.1c00614, 2021.
- 843 Yang, Y., Li, X., Shen, R., Liu, Z., Ji, D., and Wang, Y.: Seasonal variation and  
844 sources of derivatized phenols in atmospheric fine particulate matter in North China  
845 Plain, *Journal of Environmental Sciences*, 89, 136-144,  
846 <https://doi.org/10.1016/j.jes.2019.10.015>, 2020.
- 847 Zhang, B., Shen, Z., He, K., Sun, J., Huang, S., Xu, H., Li, J., Ho, S. S. H., and  
848 Cao, J.-j.: Insight into the Primary and Secondary Particle-Bound Methoxyphenols and  
849 Nitroaromatic Compound Emissions from Solid Fuel Combustion and the Updated  
850 Source Tracers, *Environmental Science & Technology*, 57, 14280-14288,  
851 10.1021/acs.est.3c04370, 2023.
- 852 Zhang, Y.-L. and Cao, F.: Fine particulate matter (PM<sub>2.5</sub>) in China at a city level,  
853 *Scientific Reports*, 5, 14884, 10.1038/srep14884, 2015.